

Tannecia S. Stephenson*, and A. Anthony Chen
University of the West Indies, Kingston 7, Jamaica

1. INTRODUCTION

Study of the interannual variability of Caribbean climate has been conducted extensively since the late 1900s. Hastenrath (1976) investigated anomalous characteristics of the general circulation in the tropical Atlantic and eastern Pacific oceans that were associated with precipitation in Central America and the Caribbean. He proposed that the equatorial Pacific was warm during a deficient mean rainy season in the region, but cold in the winter preceding it. Enfield (1996) confirms this relationship for a mean rainfall season, bolstering the idea of tropical Pacific modulation of Caribbean rainfall.

Enfield and Mayer (1997) investigated the spatial and seasonal nature of the El Niño-Southern Oscillation (ENSO) connection with the tropical Atlantic, and deduced that Pacific ENSO is strongly correlated with boreal spring SST anomalies in the tropical North Atlantic (TNA) along 10°-20°N and just north of ITCZ. They showed that winter equatorial Pacific warmings preceded those of the TNA by four to five months. Chen et al. (1997) and Giannini et al (2000) point out a relationship between the increased spring TNA SSTs and heightened early season (May-July) rainfall amounts throughout the Caribbean and Central American region, implying that the tropical Atlantic is also a significant influence on Caribbean rainfall.

It is therefore not surprising that Chen et al. (2001) found a relation between the leading PCA mode of May-June-July (MJJ) precipitation and both the wintertime Pacific sea surface temperature anomalies (SSTA) and concurrent Caribbean SSTA south of 20°N. A similar link between Caribbean rainfall and SST anomalies in both oceanic basins was also observed by Enfield and Alfaro (1999).

Our investigation seeks to identify the dominant modes of Caribbean precipitation variability on an interannual timescale that are related to SST anomalies in both the tropical Atlantic and Pacific oceans. The aim then is to confirm some of the relationships found above. As opposed to the above papers however, we divide the year into two-month periods prior to conducting our analysis, in an attempt to also investigate how the strength of the SST-precipitation associations changes as the year evolves. Section 2 describes the datasets and the methodologies used. Some results and conclusions follow in sections 3 and 4 respectively.

2. DATASETS AND METHOD

2.1 Datasets

The precipitation data (PRECIP) was compiled from the Magaña Dataset (MD) (Magaña et al., 1999) for the interval January 1958-December 1998. MD is a monthly precipitation dataset on a 0.5°×0.5° grid developed from station data and satellite estimates. It covers the Caribbean and near Caribbean region (7°-25°N, 60°-90°W), and anomalies were computed by removing the climatology. The data was then aggregated into bi-monthly averages commencing with January-February on a 1.5°×1.5° grid.

The SST database was the Reynolds Optimum Interpolated SST (Reynolds, 1988) which has a 2°×2° resolution and encompasses the region 44.5°S-59.5°N and 180°W-180°E. Two smaller SSTA datasets were extracted for the tropical Pacific (180°-80°W; 10°S-30°N) and north tropical Atlantic (90°W-0°; 5°S-27°N) oceans and averaged bi-monthly.

2.2 Method

To isolate the important coupled modes of SSTA and precipitation and the patterns of covariability of the two fields, canonical correlation analysis (CCA) is employed. CCA decomposes the eigenvector of the cross-correlation matrix between two input variables - in this case between SSTA and PRECIP - into modes of decreasing explained cross-correlation between the two analysed fields. Each mode is represented by two singular vectors describing the spatial patterns of weights for the two variables, and two series of expansion coefficients describing the weighting of the mode on the two variables in the temporal domain. As part of the analysis a matrix of M years × N grid points was separately constructed for the anomalous rainfall and SST fields for each bi-monthly interval and principal component analysis (PCA) (Kutzbach 1967, Wallace et al. 1992) applied. PCA is employed here as a prefilter to CCA to decrease random sampling fluctuations as a result of short time series (Barnett et al. 1987 Bretherton et al. 1992). The eigenmodes are retained using the scree test (Cattell, 1966) and further separated using North's rule (North et al., 1982) such that their sampling errors do not overlap. We then combine these modes separately in CCA.

For each two-month period CCA is done for the Caribbean PRECIP dataset and each of the two tropical SSTA datasets, given the associations previously noted with each. Therefore for Jan-Feb we perform CCA for both PRECIP&Atlantic SSTA and PRECIP&Pacific SSTA, with this repeated for subsequent two-month periods. We present as our diagnostic heterogeneous correlation maps i.e. the expansion coefficients of one field correlated with the grid point values of the other field, as they isolate the spatial patterns associated with

* Corresponding author address: Tannecia S. Stephenson, Dept. of Physics, Univ. of the West Indies, Mona, Jamaica; e-mail tannysyd@yahoo.com

a given mode (Wallace et al. 1992, Bretherton et al. 1992).

Only the first two modes are retained for each analysis, and the expansion coefficients of the SSTA fields for the Pacific and Atlantic are correlated with Niño-3 (5°S-5°N; 150°-90°W) and TNA (6°-22°N; 60°-15°W) SSTA indices respectively. These we consider proxies for Pacific and Atlantic variability, and the correlation enables us to characterize the extracted modes. Correlation coefficients were computed for concurrent periods as well as lags of up to six months.

For all correlations the random phase method was used to assess statistical significance at the 95% level (Ebisuzaki, 1997), while our statistical package of choice for the CCA is CLIMLAB2000[‡].

3. RESULTS

3.1 ENSO variability and Caribbean rainfall

Our discussion is confined to the leading modes of Atlantic (A1) and Pacific (P1) variability for each 2-month period. The relation between the expansion coefficients of the leading modes and climatic indices is summarized in Table 1.

For all 2-month periods, excepting May-June, P1 strongly correlates with the Niño-3 index even up to 6-months lag (Table 1(a)). Hence P1 in these months (i.e. excepting May-June) is considered an ENSO mode. Both Table 1(a) and the heterogeneous maps show that ENSO connected variability is strongest in the region during the dry Caribbean season (Nov-April) and particularly in the boreal winter months (Jan-Feb). The heterogeneous maps for Jan-Feb (Fig. 1) is characteristic of the pattern of the association, showing that strong correlations exist between SST anomalies in the equatorial Pacific and precipitation in the southwestern Caribbean basin, as well as in the northern end (north of 20°N) of the basin. Correlations in the north and south basin are however oppositely signed indicating that whereas El Niño occurrences make for a drier south Caribbean during the winter months, they also result in the north Caribbean being wetter. In Mar-Apr the magnitude of spatial coverage of ENSO related precipitation decreases, becoming more confined to the Leewards and the higher latitudes of the northern Caribbean. By May-Jun the equatorial Pacific influence disappears (c.f. Table 1(a)) and a homogenous central Caribbean basin with negative precipitation anomalies is obtained.

A weak El Niño related drying of the south Caribbean reemerges in Jul-Aug but by Nov-Dec the ENSO influence is again increasingly apparent, as a basin of oppositely signed rainfall anomalies in the northern and southern Caribbean is once again obtained.

3.2 Atlantic Variability and Caribbean Precipitation

A1 in many ways mirrors P1, as it similarly exhibits high correlations with the Niño-3 index (up to 6 months lag) for all bi-monthly periods, again with the exception of May-Jun (Table 1(b)). Recalling that the equatorial Pacific has a lagged signal in the TNA (Enfield and Mayer 1997), we conclude from the strong A1-ENSO winter correlations that for these months A1 is a proxy of Pacific variability, i.e. representing the known winter ENSO effect on the TNA. We therefore effectively obtain two winter ENSO modes as a result of the separation of the Atlantic and Pacific basins in our analysis.

Consistent with the above findings is the similarity between the A1 heterogeneous SST on precipitation map obtained for Nov-Dec (not shown) and that shown in Fig. 1a for P1. The oppositely signed north-south Caribbean signal is also evident in the winter Atlantic mode. The associated heterogeneous precipitation on SST map (Fig. 2b) also shows the beginning of a warming off the coast of Africa, consistent with a developing winter/spring TNA anomaly due to warm winter equatorial Pacific.

Table 1. Lag correlations of primary modes retained using CCA and relevant global indices. (a) P1 and Niño-3 (b) A1 and Niño-3; (c) A1 and TNA. Values in bold are significant.

| (a) | Lags (month) | | | | | |
|---------|--------------|--------------|--------------|--------------|--------------|--------------|
| P1 | 0 | 2 | 3 | 4 | 5 | 6 |
| Jan-Feb | -0.91 | -0.88 | -0.89 | -0.89 | -0.84 | -0.79 |
| Mar-Apr | -0.87 | -0.66 | -0.58 | -0.57 | -0.59 | -0.59 |
| May-Jun | -0.08 | -0.40 | -0.41 | -0.36 | -0.34 | -0.38 |
| Jul-Aug | -0.66 | -0.39 | -0.13 | 0.13 | 0.29 | -0.37 |
| Sep-Oct | -0.66 | -0.66 | -0.67 | -0.68 | -0.67 | -0.59 |
| Nov-Dec | -0.81 | -0.87 | -0.85 | -0.82 | -0.81 | -0.78 |

| (b) | Lags (month) | | | | | |
|---------|--------------|-------------|-------------|-------------|-------------|-------------|
| A1 | 0 | 2 | 3 | 4 | 5 | 6 |
| Jan-Feb | 0.88 | 0.85 | 0.85 | 0.84 | 0.79 | 0.73 |
| Mar-Apr | 0.78 | 0.53 | 0.44 | 0.43 | 0.46 | 0.48 |
| May-Jun | -0.21 | 0.05 | 0.20 | 0.30 | 0.35 | 0.33 |
| Jul-Aug | 0.51 | 0.47 | 0.30 | 0.10 | -0.01 | -0.08 |
| Sep-Oct | 0.52 | 0.54 | 0.55 | 0.54 | 0.50 | 0.45 |
| Nov-Dec | 0.77 | 0.76 | 0.73 | 0.71 | 0.71 | 0.61 |

| (c) | Lags (month) | | | | | |
|---------|--------------|--------------|-------------|-------------|-------------|-------------|
| A1 | 0 | 2 | 3 | 4 | 5 | 6 |
| Jan-Feb | 0.31 | 0.22 | 0.41 | 0.42 | 0.27 | 0.16 |
| Mar-Apr | 0.24 | 0.20 | 0.09 | 0.15 | 0.32 | 0.45 |
| May-Jun | 0.51 | 0.56 | 0.50 | 0.38 | 0.20 | 0.07 |
| Jul-Aug | -0.60 | -0.36 | -0.26 | -0.22 | -0.22 | -0.24 |
| Sep-Oct | 0.93 | 0.73 | 0.62 | 0.55 | 0.48 | 0.42 |
| Nov-Dec | 0.21 | 0.38 | 0.28 | 0.15 | 0.09 | 0.10 |

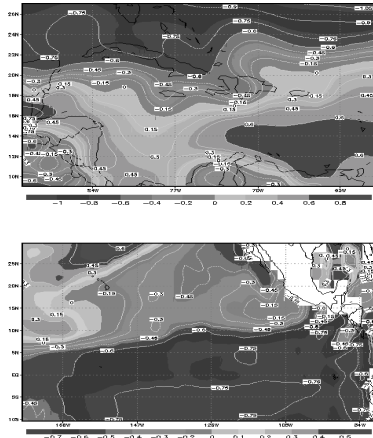
3.3 Early Season Precipitation

The disappearance of ENSO modulated rainfall for the May-Jun period (c.f. Table 1a and b) is fascinating. The decreased El Niño effect gives rise to a robust association between the TNA and Caribbean precipitation. During May-June and for the next 2 bi-monthly periods there are significant correlations between A1 and the TNA i.e. there is strong TNA

[‡] CLIMLAB2000 is an IRI (International Research Institute for Climate Prediction) statistical package.

association with the Caribbean wet season (May-Oct) (Table 1c). Fig. 2 gives the heterogeneous maps for A1 for May-June. They indicate that changes in precipitation in the main Caribbean basin during the early rainfall season are associated with TNA anomalies between 0° and 18°N.

Figure 1 Heterogeneous correlation maps for CCA mode 1 during Jan-Feb. The top panel shows the distribution of scalar correlation between gridded PRECIP anomalies and mode 1 expansion coefficients for Pacific SSTA. The bottom panel shows the distribution of scalar correlation between gridded SSTA anomalies and mode 1 expansion coefficients for PRECIP.

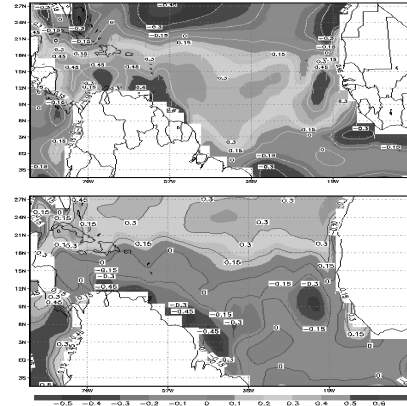


Though no concurrent relationship exists between *niño*-3 and May-June rainfall, there is evidence of a relationship four to six months prior. Note the significant correlations between A1 and ENSO (Table 1(b)) during May-June at 4-6 months lag. The idea is that the TNA is significant for modulating May-Jun rainfall but changes in the TNA during the spring months can result from equatorial Pacific SST anomalies some months earlier. This again is consistent with the findings of Enfield and Mayer (1997) and bodes well for predicting anomalously wet or dry early rainfall seasons.

4. CONCLUSIONS

We deduce that from Nov-April (the Caribbean dry season) and to a lesser extent during Sept-Oct (the latter half of the wet season) ENSO appears to be a major mode of variability in the Caribbean. The El Niño effect on rainfall is manifested as oppositely signed precipitation anomalies in the northern and southern Caribbean, the latter being negatively signed. This pattern is strongest during the boreal winter months (Nov-Dec). Caribbean rainfall variability in the early rainfall season (May-June) is however influenced by the modulations in the TNA signal, with some of the variability in the TNA itself linked to ENSO variability 4-6 months earlier.

Figure 2 Heterogeneous correlation maps for CCA mode 1 during May-June. The top panel shows the distribution of scalar correlation between gridded PRECIP anomalies and mode 2 expansion coefficients for Atlantic SSTA. The bottom panel shows the distribution of scalar correlation between gridded SSTA anomalies and mode 2 expansion coefficients for PRECIP.



Acknowledgement

This work was facilitated by a grant from the Inter-American Institute for Global change research (IAI) through their PESCA initiative.

References

- Barnett, T. P., and R. W. Preisendorfer, 1987: Origins and levels of monthly and seasonal forecast skills for the United States surface air temperatures determined by canonical correlation analysis. *Mon. Wea. Rev.*, **115**, 1825-1850.
- Bretherton, C.S., C. Smith and J.M Wallace, 1992: An Intercomparison of methods for finding coupled patterns in climate data. *J Climate*, **5**, 541-560.
- Cattell, R. B., 1966: The scree test for the number of factors. *Multivariate Behavioral Research*, **1**, 245-276.
- Chen, A. A., and M. Taylor, 2001: Investigating the link between early season Caribbean rainfall and the El Niño+1 year. (accepted for Publication. *Int. J. Climatology*).
- Ebisuzaki, W., 1997: A Method to estimate the statistical significance of a correlation when the data are serially correlated. *J Climate*, **10**, 2147 - 2153.
- Enfield, D. B., 1996: Relationships of inter-American rainfall to tropical Atlantic and Pacific SST variability. *Geophys. Res. Letters*, **23**, 3305-3308.
- Enfield, D.B., and D. A. Mayer, 1997: Tropical Atlantic sea surface temperature variability and its relation to El Niño-Southern Oscillation. *J. Geophys. Res.*, **102**, 929-945.
- Enfield, D.B., and E. J. Alfaro, 1999: The dependence of Caribbean rainfall on the interaction of the tropical Atlantic and Pacific Oceans. *J. Climate*, **12**, 2093-2103.
- Giannini, A., Y. Kushnir, and M. A. Cane, 2000: Interannual Variability of Caribbean Rainfall, ENSO and the Atlantic Ocean. *J. Climate*, **13**, 297-311.
- Hastenrath, S., 1976: Variations in low-latitude circulation and extreme climatic events in the tropical Americas. *J. Atmos. Sci.*, **33**, 202-215.
- Kutzbach, J. E., 1967: Empirical eigenvectors of sea-level pressure, surface temperature and precipitation complexes over North America. *J. App. Met.*, **6**, 791-802.
- Magaña, V., J. A. Amador, and S. Medina, 1999: The midsummer drought over Mexico and Central America. *J. Climate*, **12**, 1577-1588.
- North, G.R., T. L. Bell, F. Cahalan, and F. J. Moeng, 1982: Sampling errors in the estimation of empirical orthogonal functions. *Mon. Wea. Rev.*, **110**, 699-706.
- Wallace, J. M., C. Smith, and C. S. Bretherton, 1992: Singular Value Decomposition of wintertime sea surface temperature and 500-mb height anomalies. *J. Climate*, **5**, 561-576.